Characterization of the TE Dependence of IVIM Biomarkers in a Flow Phantom and *In Vivo*

G. Y. Cho[1], D. K. Sodickson[1], and E. E. Sigmund[1]
[1]Center for Biomedical Imaging - Radiology, NYU School of Medicine, NEW YORK, New York, United States

Introduction: Intravoxel incoherent motion (IVIM) is a scheme of sampling and analysis of diffusion-weighted imaging (DWI) data producing biomarkers of both tissue structure and vascularity [1]. Recently, its application has grown in highly vascular organs and pathologies [2-5]. However, far less attention has been given to possible dependences of IVIM biomarkers on experimental sequence timing. Recent observations have shown echo time (TE) dependence of pancreatic perfusion fraction, attributable to differential relaxation weighting [6]. Furthermore, there may be dependence of the apparent pseudo-diffusion (D_p) rate on observation time when such times are similar to transit times for a typical vessel branch [7-8]. With the proper sampling and modeling, this dependence could be exploited for more specific quantification of both vessel geometry (e.g. segment length) and blood velocity. In highly vascular organs such as in renal tissue, this specificity may aid in parsing vascular and tubular flow contributions to DWI. Within malignant tumors, the ability to separately monitor vascular geometry and dynamics would also be valuable, especially during anti-angiogenic treatments. With this motivation in mind, the dependence of IVIM parameters upon TE was explored in a flow phantom as well as in kidney *in vivo* in a full body clinical scanner.

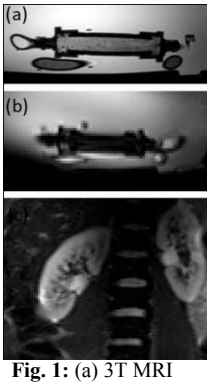

Fig. 1: (a) 3T MRI phantom (b) DWI image (c) Coronal b0 image of kidney

Methods: A previously developed IVIM flow phantom was used where flow was pumped into a sponge simulating a complex capillary network [9]. Measured pressure difference (ADInstruments) of 12 mmHg at proximal and distal ends of the sponge was used as a surrogate flow marker. Both phantom and kidney scans were collected in a full body Siemens 3T Verio, using body and spine receiver arrays. For the phantom, a twice refocused spin echo (TRSE) sequence with bipolar gradients and axial echo planar imaging (EPI) readout was used (TR=3000 ms, matrix 128x80x3, resolution 2.6x2.6x4.8 mm) with up to 16 diffusion weightings between 0<b<600 s/mm^2, and 3 orthogonal diffusion directions (x,y,z). 5 TE values were used (68, 90, 105, 120, 150 ms). A coronal kidney IVIM DWI scan using TRSE-EPI with prospective gating via phase scout was performed on one healthy subject (TR=5167 ms, matrix 156x192x6, resolution 2.2x2.2x6 mm, 5 avgs). Images were collected at 9 b values between 0<b<600 s/mm^2, 3 orthogonal directions which were averaged, and 3 TE values (78, 100, 120 ms). Similar to previous work on IVIM in the phantom and *in vivo* [9-11], ROI signal decay curves derived from (1) static bath fluid, (2) flow phantom with/without flow, and (3) renal cortex were analyzed with a bi-exponential model:

$$M_i = M_0 \cdot [(1 - f_P) \cdot \exp(-b_i \cdot D_t) + f_P \cdot \exp(-b_i \cdot D_p)]$$

where f_p is perfusion fraction, D_p is pseudodiffusivity, and D_t is tissue diffusivity. The total flux parameter f_p*D_p was considered [12]. A monoexponential model was used to extract apparent diffusion coefficient (ADC). The dependence of the IVIM biomarker with TE was measured in each case.

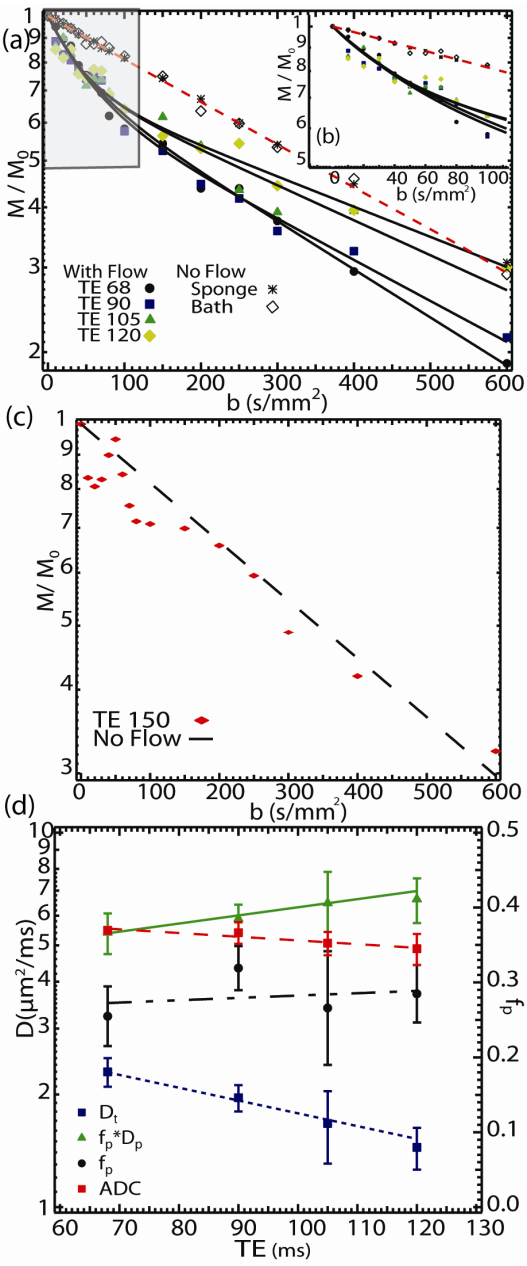

Fig. 2: (a,b) Phantom ROI DWI decays (c) High TE oscillations in ROI decay (d) IVIM biomarkers vs. TE

Results: Fig. 2a shows phantom ROI decay curve results at 4 different TE values. Initial observation shows signal attenuation lessens with increasing TE. Closer inspection (Fig. 2b) shows a faster rate of decay at higher TE for low b values (<50s/mm^2). Signal oscillations with b-value are observed in all decay curves, especially pronounced at higher TE (Fig. 2c). In Fig. 2d, IVIM analysis versus TE shows increasing f_p*D_p and decreasing D_t with increasing TE. ADC and f_p are nearly constant as a function of TE during flow. Fig. 3a shows kidney results of ROI decay at various TE with slightly increasing amount of decay as TE increases. In Fig. 3b, IVIM markers with respect to TE show an increasing trend for f_p and f_p*D_p while D_t remains constant.

Discussion: Previous experiments with the phantom show D_p can be considered as a flow marker [9-11]. In both phantom and kidney results, the f_p*D_p dependence on TE may, in theory, be related to flow dynamics as the time regime of the spins passing through networks approaches the TE of the sequence. The inverse relationship between D_t and TE seen in the phantom likely is a result of the oscillating decay as the signals at higher b values (which strongly influence D_t) reach a peak in the wave. The source of these oscillations may be the pulsatile flow of the peristaltic pump causing constructive/destructive interference when its period (50 ms) is of order TE [13]. Also, previous literature has shown pancreatic f_p dependence on TE because of differential relaxation weighting [6]; preliminary results suggest similarities in the *in vivo* kidney results as f_p increases with TE. Finally, the constant ADC shows it is a less specific indicator that fails to separate characteristics of diffusion and flow. In this work, dependences exists between certain IVIM biomarkers and TE, which in combination with IVIM modeling for arbitrary gradient waveforms [7-8] may allow extraction of characteristics of the vasculature. Tumor vasculature has been noted to possess sluggish flow and complex vasculature compared to normal capillaries. These properties, along with anti-angiogenic therapy, could be tracked with a TE-dependent IVIM protocol. Thus, each application in which IVIM provides vascular/cellular biomarkers may be further amplified by the controlled variation of sequence timing. While this preliminary data is promising, more comprehensively sampled and statistically validated data, especially *in vivo*, is required before determining robust experimental trends and developing advanced modeling.

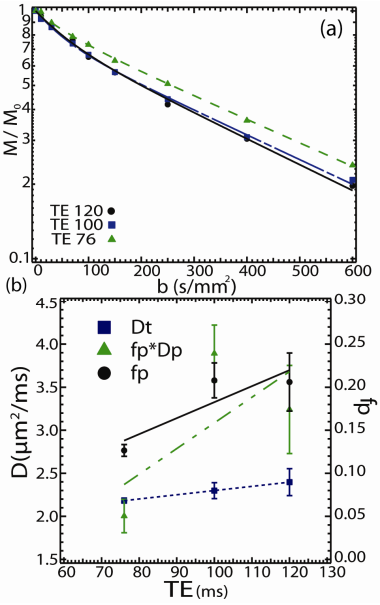

Fig. 3: (a) Renal cortex ROI DWI decay curves (b) IVIM biomarkers versus TE.

Ref: [1]Le Bihan. Radiol, 1986. **161**(2): p.401-7.[2]Lemke. Invest Radiol, 2009. **44**(12): p.769-75.[5]Luciani. Radiol, 2008. **249**(3): p.891-9.[4]Zhang. Radiol, 2010. **254**(3): p.783-92.[5]Eisenberger. **20**(6): p.1374-83.[6]Lemke. MRM, 2010.[7]Kennan. Med Phys, 1994. **21**(4): p.539-45.[8]Gao. Med Phys, 1988. **15**(6): p.809-14.[9]ISMRM 2010:2723[10]ISMRM. 2010:2779[11]ISMRM. 2010:364[12]Le Bihan. MRM, 1992. **27**(1): p.171-8.[13]Sigmund. JMR, 2001. **148**(2): p.309-13.